ACS OMEGA

http://pubs.acs.org/journal/acsodf

Article

Identification of Thermostable Xylose Reductase from *Thermothelomyces thermophilus*: A Biochemical Characterization Approach to Meet Biofuel Challenges

Nabeel Ali, Ayesha Aiman, Anas Shamsi, Imtaiyaz Hassan, Mohammad Shahid, Naseem A. Gaur, and Asimul Islam*

Cite This: *ACS Omega* 2022, 7, 44241−44250

Read Online

ACCESS | Metrics & More | Article Recommendations | Supporting Information

ABSTRACT: The constant rise in energy demands, costs, and concerns about global warming has created a demand for new renewable alternative fuels that can be produced sustainably. Lignocellulose biomass can act as an excellent energy source and various value-added compounds like xylitol. In this research study, we have explored the xylose reductase that was obtained from the genome of a thermophilic fungus *Thermothelomyces thermophilus* while searching for an enzyme to convert xylose to xylitol at higher temperatures. The recombinant thermostable TtXR histidine-tagged fusion protein was expressed in *Escherichia coli* and successfully purified for the first time. Further, it was characterized for its function and novel structure at varying temperatures and pH. The enzyme showed maximal activity at 7.0 pH and favored D-xylose over other pentoses and hexoses. Biophysical approaches such as ultraviolet−visible (UV−visible), fluorescence spectrometry, and far-UV circular dichroism (CD) spectroscopy were used to investigate the structural integrity of pure TtXR. This research highlights the potential application of uncharacterized xylose reductase as an alternate source for the effective utilization of lignocellulose in fermentation industries at elevated temperatures. Moreover, this research would give environment-friendly and long-term value-added products, like xylitol, from lignocellulosic feedstock for both scientific and commercial purposes.

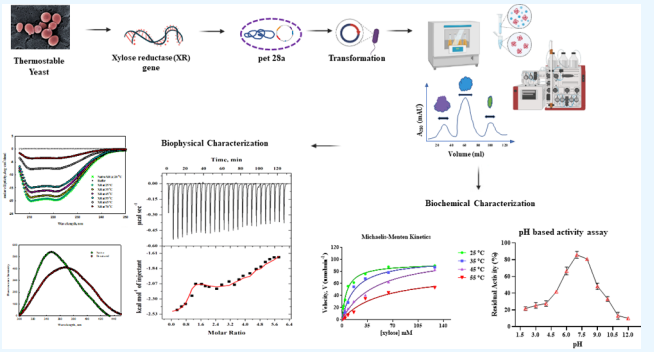

1. INTRODUCTION

The depletion of fossil fuel reserves, the economic difficulties connected with their usage, and rising environmental concerns about greenhouse gas emissions have prompted a quest for alternative energy sources that are renewable in nature.[1] Because lignocellulosic biomass is globally considered one of the most abundant renewable biomass sources,[2] and its use does not compete with food production on land, it has emerged as a viable alternative to fossil fuels for biofuel production and value-added commodities.[3,4] Lignocellulose has a complex three-dimensional network model. It is predominantly composed of a branched and amorphous carbohydrate polymer of hemicellulose (∼20−34%), a linear and crystalline carbohydrate polymer of cellulose (∼31−51%), and an aromatic polymer of lignin (∼15−25%).[5,6] Cellulose is a monomer of glucose linked by β (1 → 4) glycosidic bonds, while hemicellulose is a branched and complex polymer of galactose, xylose, and arabinose.[7] Xylose, an aldopentose sugar, can be metabolized or fermented by Archaebacteria, Clostridia, Proteobacteria, yeasts, and some filamentous fungi, and is a substantial component of lignocellulosic biomass.[6,8] However, because of carbon catabolite suppression, most organisms, including *Escherichia coli*, are unable to successfully utilize both glucose and xylose at the same time.[9] Repression of carbon catabolite leads to inefficient fermentation processes in which glucose is used, and xylose remains unutilized. As a result, there is a lot of interest in identifying or creating novel strains that can use xylose sugar effectively enough to meet the rising demands of bioethanol. Therefore, thermophilic organisms such as *Thermothelomyces thermophilus* (Tt) provide additional benefits in lignocellulosic carbon source fermentations.[10] Tt belongs to the category of ascomycetes, which prefer to grow at higher temperatures (45−55 °C).[11] These fungi possess heat-loving characteristics and cannot thrive below 20 °C. Tt fungi have been considered safe and cheap for large-scale manufacturing methods and have been utilized effectively in metabolic engineering.[12]

Received: September 2, 2022
Accepted: November 4, 2022
Published: November 17, 2022

Recently, xylose reductase (XR) has attracted considerable scientific attention from various researchers across the globe because of its ability to catalyze pentose sugars, mainly xylose to xylitol.[13] Effective utilization of xylose is important as D-xylose accounts for about 35% of the whole sugar present in lignocellulosic hemicellulose biomass.[14] Conversion of lignocellulosic xylose to xylitol is the very first and rate-limiting step in xylose metabolism, with xylitol further being converted into xylulose in the presence of enzyme xylitol dehydrogenase; eventually, bioethanol is formed via the pentose phosphate pathway.[15] Xylitol is one of the low-calorie sugars used in pharmaceuticals, beverages, and food industries.[16] Xylitol consists of approximately 400 million USD of market per year, which is further expected to double in coming years (by the end of 2025).[17] Although various reasonable chemical methods are available for xylitol production, enzymatic catalysis is always preferred over any other artificial methods available due to the eco-friendly origin of the final product and long-term sustainability.[18]

XR is mainly present in yeasts and filamentous fungi. So far, the most reported and well-characterized fungus (having active XR genes) is not promising enough in terms of efficient xylose metabolism to xylitol and bioethanol production. This can be attributed to a lack of enzyme efficiency in industrial fermentation conditions like extreme pH and temperatures.[19] There are several nonconventional fungal species present in nature that are not yet studied,[20,21] although these fungi might be proven as the source of stable enzymes.[21]

Heat-stable XRs can be easily directed to utilize heat-treated lignocellulosic biomass for xylitol formation from xylose,[22] and xylose, which is a type of reduction reaction and, at the same time, one of the cofactors of XR that is either NADH or NADPH, gets oxidized.[7] Because lignocellulosic waste is plentiful and renewable, biological processes that use xylose-rich lignocellulosic hydrolysates to act as a carbon source can reduce significantly lower raw material costs while also assisting with overall sustainability.

Therefore, in this study, the XR gene was identified from the genome of *T. thermophilus* to find a novel XR protein having high activity at elevated temperatures. After successful expression and purification of XR from *T. thermophilus* (TtXR), biochemical characterization at different temperatures and pH was performed. The structural integrity of the purified TtXR was also studied using biophysical methods, i.e., ultraviolet−visible (UV−visible), fluorescence, and far-UV CD spectroscopies. This research has a potential application in the fermentation industry as an alternate source of XR for lignocellulose biomass usage at higher temperatures.

2. RESULTS AND DISCUSSION

2.1. Protein Expression and Purification. As recombinant TtXR was histidine-tagged, therefore immobilized metal affinity chromatography (IMAC) was employed for purification. Various growth conditions were checked and fine-tuned, and we found that at a temperature of 37 °C for 5 h, maximum protein expression was obtained compared to the one obtained at 20 °C for 12 h (Supporting Figure S1). The best induction concentration of isopropyl β-D-1-thiogalactopyranoside (IPTG) used for maximum expression was found to be 0.15 mM and this was taken as the final concentration. The total amount of the protein obtained in each step of purification is summarized in Table 1. The enzymatic activity of the xylose reductase was measured throughout the purification process for both specific activities and purification yield determination.

Table 1. TtXR Purification Using His-Tag[a]

steps involved	fraction volume (mL)	total activity of protein (U)	specific activity (U mg^{-1})	total protein recovered (mg)	yield (%)
crude soluble fraction	53.7	25.6	0.8	52.8	100
purified TtXR	17.7	12.8	2.7	6.4	38.2

[a]The activity of XR in crude and purified forms was measured in a reaction mixture containing 150 mM xylose and 0.25 mM NADPH at 7.0 pH.

The purity of the protein was checked using sodium dodecyl sulfate polyacrylamide agarose gel electrophoresis (SDS-PAGE).[23] SDS-PAGE is considered a simple and effective technique in biochemistry, employed to determine the purity and the size of the protein molecule.[23] Proteins eluted with 50, 100, and 150 mM imidazole concentrations showed a major band of the protein of interest (Supporting Figure S2). It may be noted that a faint additional protein band (few impurities), was later removed using gel filtration chromatography (inset of Figure 1). The apparent molecular weight of purified TtXR with the histidine tag was 37.8 kDa, which was very close to the theoretically predicted molecular weight of xylose reductase.[24] The molecular weight of the protein was confirmed by running 5 μL of the known molecular weight protein marker to the next well in the same 12% gel (Figure 1).

2.2. Enzyme Kinetics and Substrate Specificity. The activity of the purified and crude soluble fractions of cell-free lysate was checked using UV−visible spectroscopy. Specific activity was measured with respect to different substrates, and maximal specific activity was observed toward xylose. Also, another C_5 sugar, adonitol, showed significant activity. However, it showed significantly less activity for sucrose and sorbitol, which confirmed the affinity of xylose reductase more toward C_5 sugars (Figure 2A). Further, the kinetics of the purified protein were measured using different substrate concentrations. It can be seen from Figure 2B that with every increase in substrate (xylose) concentration, the percentage saturation of the enzyme active site increased, which was confirmed by changes in the absorbance at 340 nm. Protein concentration in the purified XR sample was kept constant at around 18−20 μM. The addition of xylose in the reaction mixture was continued till the maximum velocity of the enzyme or complete saturation of the enzyme binding site for catalysis was attained (Figure 2B). From Figure 1, we may say that we obtained the purified protein with structural integrity, as it showed decent activity with different concentrations of the substrate. The presence of activity confirmed that the purified protein adopted final folded conformation, as it performed its function. Xylose reductase from *T. thermophilus* exhibits optimal activity at 45 °C, a rare feature among XRs from other sources. This fact shall offer potential advantages during enzyme processing and ethanol production.

2.3. Characterization of Purified Recombinant TtXR. Using the enzyme kinetics of XR at different temperatures ranging from 25 to 55 °C, the optimal temperature was determined (Figure 3A). The reaction mixture was incubated

https://doi.org/10.1021/acsomega.2c05690
ACS Omega 2022, 7, 44241−44250

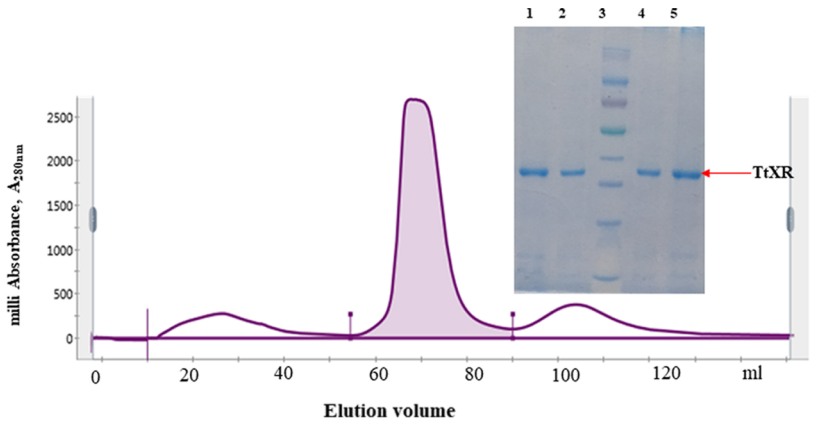

Figure 1. Size exclusion profile: chromatogram showing elution of the purified form of TtXR (inset showing the SDS-PAGE profile of the protein obtained from the peak top, loaded in lanes 1, 2, 4, and 5, and lane 3 contained 5 μL of the protein marker (10−180 kDa)).

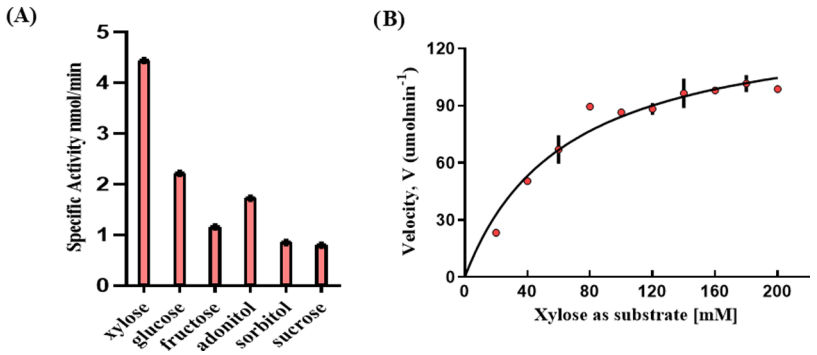

Figure 2. (A) Specific activities of TtXR toward different carbonyl substrates; (B) steady-state kinetic characterization of xylose reductase using xylose as a substrate.

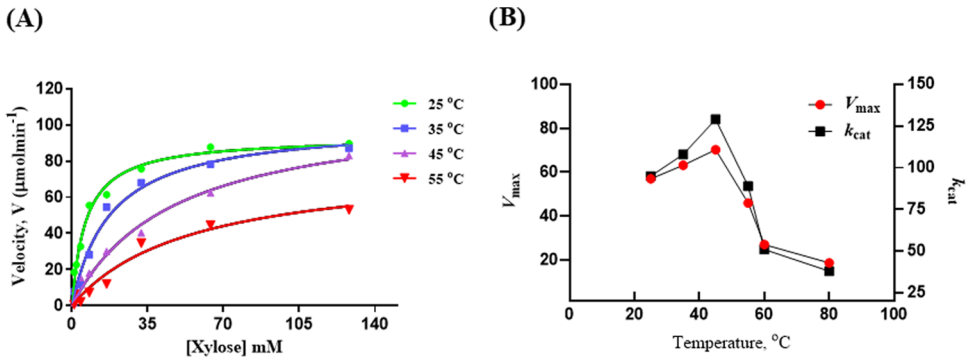

Figure 3. (A) Kinetics of purified TtXR performed at different temperatures with xylose as a substrate; (B) effect of temperature on V_{max} and k_{cat} of purified TtXR.

for at least 10 min before taking all of the measurements at different temperatures. On the basis of experiments of enzyme kinetics at different temperatures, we observed an increase in enzyme activity from 25 to 45 °C, possibly due to an increased rate of collision with an increase in temperature. But after 50 °C or above, we observed a steep fall in the activity of xylose reductase (Table 2). k_{cat} (enzyme turnover number) increased up to 45 °C, and then there was a sudden decrease in the value of k_{cat}. K_m was also calculated and compared against different temperatures (Table 2).

The optimum temperature range for yeast fermentation varies from 28 to 35 °C in industries.[25] However, we obtained the optimum activity at 45 °C (Figure 3B and Table 2). This information is very useful for industry, as this protein is stable and active in and above industrial fermentation conditions.[26] It shall provide a high yield on mass production where a rise in temperature during the process is the concern.[27] There is a loss in the activity at 55 °C, but the value of k_{cat} is 4.38, which shows that the reaction will continue even at higher

Table 2. Kinetic Parameters of TtXR at Different Temperatures

temperature (°C)	V_{max}	K_m (xylose as substrate) (mM)	k_{cat} (min^{-1})
25	93.4	6.4 ± 0.86	5.27
35	101.5	18.0 ± 3.14	5.6
45	110.8	47.0 ± 8.94	6.11
55	78.84	55.0 ± 8.51	4.38

https://doi.org/10.1021/acsomega.2c05690
ACS Omega 2022, 7, 44241−44250

temperatures, implying that the enzyme is intact at higher temperatures.

2.4. Effect of pH on Enzyme Activity. The impact of pH on enzyme activity was investigated at pH levels ranging from 2.0 to 11.0 to see the effect of various pH environments on the functional activity of TtXR. The overall charge that a protein acquires depends on the buffer conditions, which eventually affect the stability and activity of the enzyme. The pH of the intracellular condition in which the protein is present is one of the critical factors that govern the protein's native conformation and function. Thus, we performed a pH-based study to determine the optimal pH condition for maximal xylose-to-xylitol conversion. It was observed that as we go away from pH 7, the enzyme activity decreased on either side, i.e., alkaline and acidic, with maximum activity found at pH 7.0 (Figure 4).

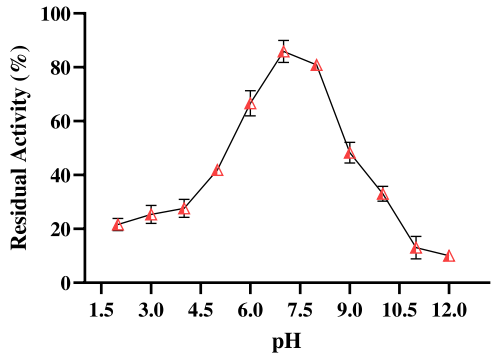

Figure 4. Xylose reductase residual activity at different pH conditions.

2.5. Biophysical Characterization of Purified TtXR. *2.5.1. Effect of Temperature on the Tertiary Structure of Xylose Reductase.* To monitor the tertiary structure of the protein, a near-UV absorbance spectrum was carried out, which showed a peak at around 280 nm, which was the signature of folded protein (Figure 5A). Further, the effect of temperature on the tertiary structure of the protein was monitored using UV−visible spectroscopy. A thermal scan was recorded at 280 nm from 20 to 85 °C. The heat-induced denatured protein obtained after the experiment was allowed to cool at room temperature and spectra showed a slight increase in the absorbance value with the shift of λ_{max} to a shorter wavelength or a blue shift.[28] We observed almost no change in absorbance at the temperature range from 20 to 50 °C. Beyond 60 °C, we clearly observed the initiation of melting or perturbation of the tertiary structure. Absorbance kept on changing up to 73 °C, and beyond that, the complete denatured state of the protein was achieved (Figure 5B). From the heat-induced transition curve, melting temperature (T_m) was determined. We observed that the melting temperature of TtXR was around 63 °C, which was very close (64 °C) to the melting temperature value obtained from the bioinformatics tool.[29] It should be noted that T_m is an index of the stability of a protein.[30] The higher the T_m, the more stable the protein.[31]

2.5.2. Effect of Temperature on the Secondary Structure of TtXR. Far-UV CD is an excellent technique to monitor the perturbation of the secondary structure of the purified protein under the influence of different pH or heat stress (temperature-based changes).[32] The secondary structure of xylose reductase was monitored using the best optimal pH condition in 50 mM sodium phosphate (at pH 7.0). The peak obtained in the far-UV CD scan at wavelengths of 222 and 208 nm indicated the dominance of the α-helix in the protein. The spectral scan was measured again from 20 to 70 °C. Spectra scan showed minimal fluctuation or loss of the secondary structure up to 50 °C. But beyond 50 °C, a decrease in the CD signal was observed, indicating the initiation of melting of the α-helix above 50 °C. The complete loss of the secondary structure was observed at 70 °C (Figure 6). It appears that upon slight heating, there is a slight loss of the structure in the protein, making it more dynamic and mobile. This slight loss in the structure may increase the activity of the protein. Changes in the environment of the residues in the active site could lead to a change in the dynamics of conformation and enhancement in its activity. This phenomenon supports the hypothesis of structure−activity trade-off.[33,34] The protein structure and enzyme activity are well-associated with each other. It seems that the stability of the active site decreases at slightly higher temperature, leading to more flexibility and hence more activity, which can be related to the well-established stability−activity trade-off.[34] Our results are consistent with this

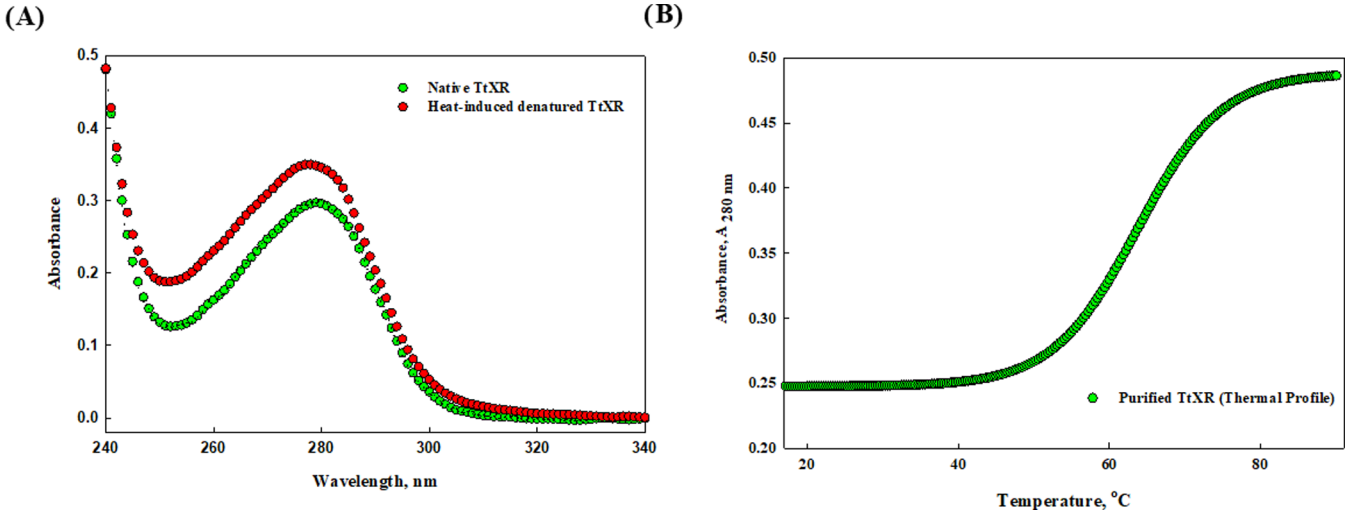

Figure 5. (A) Near-UV absorbance spectra of native vs denatured TtXR; (B) thermal spectrum of purified TtXR using UV−visible spectroscopy.

https://doi.org/10.1021/acsomega.2c05690
ACS Omega 2022, 7, 44241−44250

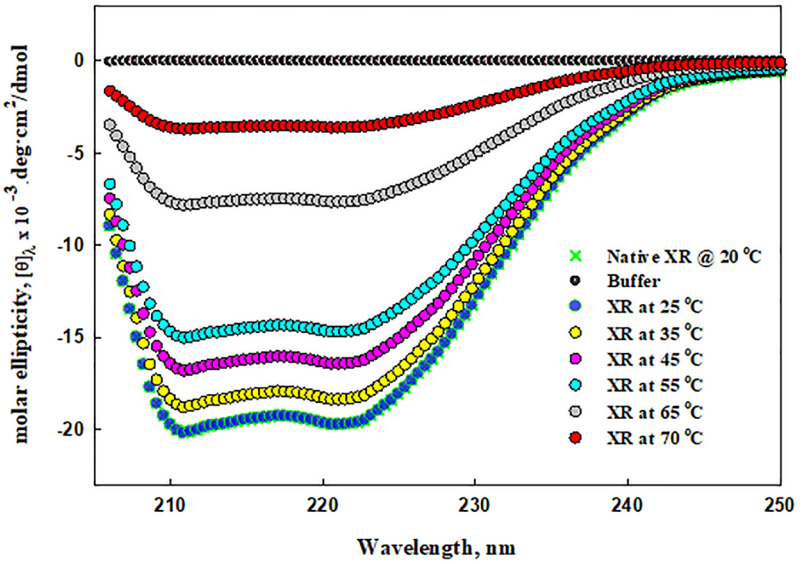

Figure 6. Effect of different temperatures on the far-UV CD spectra of purified xylose reductase.

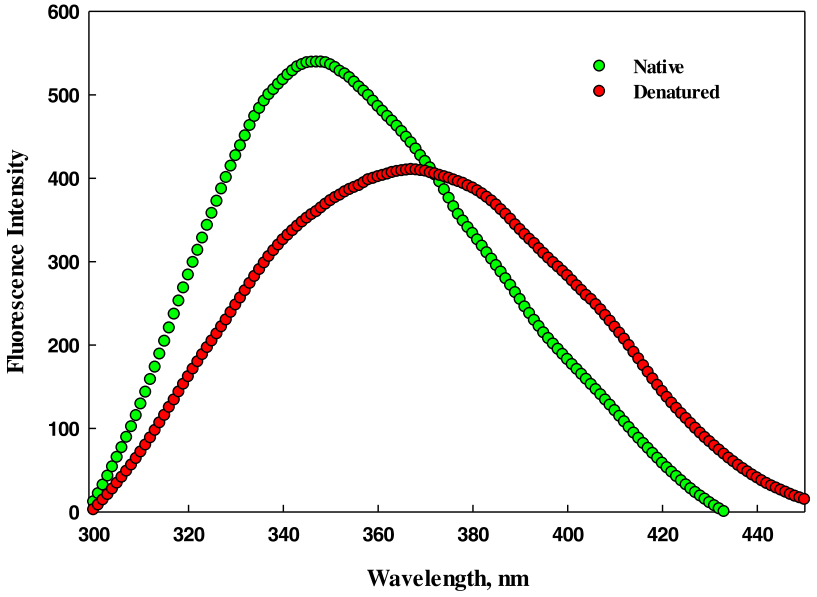

Figure 7. Comparison of fluorescence spectra of native xylose reductase vs denatured (heat-induced at 70 °C).

hypothesis. Further, an increase in temperature decreases the structure drastically and thus the activity.

2.5.3. Fluorescence Measurements. Xylose reductase contains seven Trp residues distributed all over the structure. A large number of tryptophan residues have the benefit of acting as structural integrity reporters for XR. As a result, we employed intrinsic Trp fluorescence measurements as a primary tool to investigate the structural integrity of XR. XR undergoes denaturation upon increasing the temperature; therefore, we observed a decrease in fluorescence intensity (thermally denatured), and the λ_{max} of tryptophan residues shifted toward the longer wavelength (red shift). The λ_{max} of native protein spectra was at around 347 nm, whereas after heat-induced denaturation, the λ_{max} of the protein shifted towards a longer wavelength (366 nm; Figure 7). These observations indicate that tryptophan residues are transferred from a nonpolar environment to a polar milieu or that the unfolding of the protein is observed.[35,36]

2.6. Isothermal Titration Calorimetry (ITC). Isothermal titration calorimetry (ITC) measurements were performed to know the binding affinity of xylose with the purified TtXR. ITC is a widely used technique to deduce the interactions between proteins and other molecules based on changes in energy when the two moieties or molecules bind to one another.[37] Figure 8 depicts the graphical outcomes of titrated xylose with the protein, TtXR. Calorimetric responses owing to consecutive injections of xylose in the sample cell with the protein are shown in the upper section, while the lower section depicts integrated heats of interactions as a function of the [xylose]/[xylose reductase] molar ratio (Figure 8). The top panel in the figure gives the raw data in power vs time (heat per unit of time liberated from every injection of the ligand with respect to the protein), while the lower panel in the figure displays the raw data in power standardized to the amount of the injectant (kcal mol^{-1}) vs its molar ratio of ligand injections into the cell containing xylose reductase. From the data, the

https://doi.org/10.1021/acsomega.2c05690
ACS Omega 2022, 7, 44241−44250

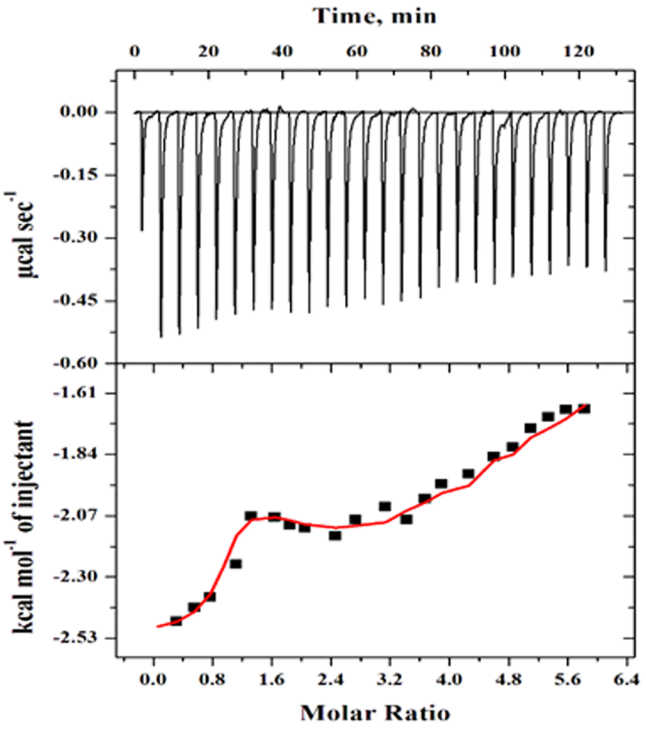

Figure 8. Isothermal titration calorimetry (ITC) profile of TtXR−compound binding.

thermodynamic binding parameters were calculated, showing the change in enthalpy (ΔH), association constant (K_a), equilibrium dissociation constant, and change in free energy ($\Delta G°$), which was estimated using the equation given below. From Table 3, it can be observed that $\Delta G°$ is negative, signifying the spontaneity of the reaction, and negative enthalpy change means the process is exothermic in nature. It appears that the protein binds to xylose to show its activity, and the activity increases as we increase the concentration of the substrate. ITC helps us to understand the mechanism of interaction and sheds light on the change in activity as the substrate concentration and the system's temperature change.

3. MATERIAL AND METHODS

3.1. Materials. The C41 (DE3) strain of *E. coli* was used to express the protein. *E. coli* cells harboring recombinant plasmids were grown aerobically at 20 °C in Luria−Bertani (Merck, Darmstadt, Germany) broth with 50 μg mL^{-1} kanamycin (Sigma, Saint Louis, MO). Using standard procedures, plasmid isolation and competent cell preparation were carried out.[38] The substrates, xylose, glucose, sucrose, arabinose, etc., used in this study were purchased from Merck India Pvt. Ltd. Reduced nicotinamide adenine dinucleotide phosphate (NADPH), dimethyl sulfoxide (DMSO), and NADH (nicotinamide adenine dinucleotide) were bought from Sigma-Aldrich. All other reagents like phosphate buffer, Tris buffer, sodium chloride, LB agar, LB broth, SDS, etc., of analytical grades were purchased from Merck Ltd.

3.2. Expression and Purification of Xylose Reductase. A full-length *TtXR* gene integrated into pET-28a was obtained from Biomatics Ltd., India. The transformation of the plasmid into *E. coli* BL21 (DE3) was done for expression. The purification of xylose reductase present in the soluble fraction was done by affinity chromatography (immobilized metal ion chromatography). The column was first pre-equilibrated with potassium phosphate buffer (50 mM, pH 7.0) and then washed with equilibration buffer. During the process of binding at 4 °C, the flow rate of the column was kept as slow as possible (0.2 mL min^{-1}) to ensure the proper exposure of Ni-NTA column beads to the histidine-tagged protein of interest (xylose reductase).

The purification of the crude enzyme present in the soluble fraction was subjected to chromatographic techniques, namely, affinity chromatography and gel filtration, to obtain the protein of interest in its highest purity. The prepared sample having approximately 3 mL of aqueous protein (using a 3 mL loop) was poured into a Ni-NTA column pre-equilibrated with 150 mM NaCl, 5% (v/v) glycerol, 0.5 mM β-mercaptoethanol, and 5 mM imidazole. The elutions of the protein bound to the Ni-NTA column were done at different concentrations of imidazole (50−500 mM) in 50 mM potassium phosphate buffer, keeping the flow rate at 0.5 mL per min. The eluted fractions of the protein, obtained from the Ni-NTA affinity column, were concentrated to 5 mg mL^{-1} using an Amicon ultrafiltration device with a 10 kDa cutoff. After that, the concentrated protein was applied to a Superdex 200 pg column for gel filtration chromatography. The gel filtration column was pre-equilibrated with the same 50 mM phosphate buffer of pH 7.0. The protein was eluted in the equilibration buffer at a flow rate of 0.5 mL min^{-1}. The sample collection was done at 4 °C. The active fractions were pooled, dialyzed against the 50 mM phosphate buffer of pH 7.0, and concentrated.[39] The fractions (3 mL each) were collected for SDS-PAGE to check the purity of the protein obtained in each fraction. SDS-PAGE of 12% separating gel and 4% stacking gel was prepared using the method given by Laemmli 1970.[40] The previously pooled samples were prepared by adding 1% (w/v) SDS and then boiling for 5 min at 100 °C in eppendorfs. To visualize the purified protein, gel electrophoresis was run in Tris−HCl buffer of pH 8.3 at 80−100 V for 3 h. After electrophoresis, the protein bands on the gel were made detectable by staining with standard Coomassie Brilliant Blue. Samples showing the discrete band in SDS-PAGE were assayed for xylose reductase activity.[41]

3.3. Xylose Reductase Activity Assay and Data Analysis. TtXR activity was evaluated using a spectrophotometer to detect the change in A_{340} following NAD(P)H oxidation, as described in many reports of xylose reductase

Table 3. Calorimetric Binding Parameters Obtained by the Analysis of ITC Measurements on the Interaction of the Ligand with Purified Xylose Reductase at 298 K (25 °C) and pH 7.0

thermodynamic parameters (units)	step 1	step 2	step 3
K_a (M^{-1})	$7.47 \times 10^5 \pm 8.5 \times 10^4$	$1.29 \times 10^4 \pm 1.7 \times 10^3$	$2.52 \times 10^3 \pm 2.28 \times 10^2$
$\Delta H°$ (cal mol^{-1})	-2.62×10^3	-6.599×10^3	-4.24×10^4
$\Delta S°$ (cal mol^{-1}deg^{-1})	17.93	−2.94	−123.9
$\Delta G°$ (cal mol^{-1})	$-7.048 \times 10^3 \pm 90.0$	$-5.58 \times 10^3 \pm 7.73 \times 10^2$	$4.2 \times 10^3 \pm 88.0$

https://doi.org/10.1021/acsomega.2c05690
ACS Omega 2022, 7, 44241−44250

activity from other sources.[42] Unless indicated otherwise, the TtXR assay mixture (1.0 mL) for the reaction contained 100 mM phosphate buffer (pH 7.0), 200 μM NAD(P)H, 150−160 mM xylose, and enzyme solution (0.1 mL). This reaction mixture was allowed to stand for 1 min to eliminate the endogenous oxidation of NADPH, and the reaction was started by adding 0.1 mL of the substrate. One unit of enzyme activity is defined as the amount of enzyme required to oxidize 1 μmol of NADPH per min under the specified conditions. Data analysis was done using the below-mentioned equations

$$\text{volumetric activity} = \frac{\Delta\text{Abs} \times V_{\text{total}}}{\varepsilon \times V_{\text{enzyme}} \times d} \quad (1)$$

$$\text{specific activity} = \frac{\text{volumetric activity}}{c_{\text{enzyme}}} \quad (2)$$

$$k_{\text{cat}} = V_{\text{max}}/[\text{Et}] \quad (3)$$

$$\text{catalytic efficiency} = \frac{k_{\text{cat}}}{K_{\text{M}}} \quad (4)$$

$$\text{purification factor (PF)} = \frac{\text{specific activity}_{\text{fraction}}}{\text{specific activity}_{\text{crude extract}}} \quad (5)$$

$$\text{recovery (\%)} = \frac{\text{total activity}_{\text{fraction}}}{\text{total activity}_{\text{crude extract}}} \times 100 \quad (6)$$

where V_{max} is the maximum enzyme activity; K_{M} is the apparent affinity constant; ΔAbs is the change in absorption (min^{-1}); V_{total} is the assay volume (mL); ε is the extinction coefficient of NAD(P)H at 340 nm (6.22 $\text{L·mmol}^{-1}\text{·cm}^{-1}$); [Et] is the enzyme concentration used in the reaction mixture; V_{enzyme} is the volume of enzyme solution (mL of XR), and d is the path length (1 cm).

3.4. Measurement of the Thermostability of the Protein Using UV−vis Spectroscopy. Optimized temperature studies were performed using TtXR activity measurements. Further, thermal characterization of TtXR was standardized via incubation at multiple temperatures of 20−70 °C for at least 10 min before measurements. Three-dimensional structural changes were monitored over a broad range of different temperature conditions. The absorption spectra of XR protein samples preincubated with phosphate buffer 50 mM pH 7.0 were measured using a Jasco UV/visible spectrophotometer (Jasco V-660, Model B 028661152) equipped with a Peltier-type temperature controller (ETCS-761). All spectra measurements were carried out in the wavelength range of 340−240 nm using a 1 cm path length cell. Baseline correction was always done using a respective blank solution. For each measurement, a protein concentration of 0.2 mg mL^{-1} was used. After denaturation, each protein sample was immediately cooled to see the reversibility of TtXR. At least three independent measurements were performed and averaged for the analysis of each sample. The retained enzyme activity was measured as described in the xylose reductase activity assay.[43] T_{m} and thermal stability were measured by heating the purified TtXR from 20 to 90 °C. Each heat-induced transition curve was analyzed for T_{m} (midpoint of denaturation) and ΔH_{m} (enthalpy change at T_{m}) using a nonlinear least-squares analysis according to the following relation

$$y(T) = \frac{y_{\text{N}}(T) + y_{\text{D}}(T)\exp\left[-\Delta H_{\text{m}}/R\left(\frac{1}{T} - \frac{1}{T_{\text{m}}}\right)\right]}{1 + \exp\left[-\Delta H_{\text{m}}/R\left(\frac{1}{T} - \frac{1}{T_{\text{m}}}\right)\right]} \quad (7)$$

where $y(T)$ is the optical property at temperature T (K), $y_{\text{D}}(T)$ and $y_{\text{N}}(T)$ are the optical properties of the denatured and native molecules of protein at temperature T (K), respectively, and R is the gas constant.

3.5. Substrate Specificity. The substrate specificity of xylose reductase was measured by replacing 150 mM D-xylose with 150 mM D-glucose, fructose, adonitol, sucrose, D-galactose, or sorbitol as the substrate in the reaction mixture. Apart from different substrates, the rest of the assay conditions were kept the same as described in the TtXR activity assay. Finally, the prepared reaction mixture was kept for 5 min for incubation at room temperature before measurements. All of the kinetics measurements were performed in triplicates to minimize the possible error during pipetting and experimentation.

3.6. Sample Preparation for pH Measurements. pH is one of the most important factor, which decides the functionality of an enzyme to carry out a specific catalytic reaction. Purified TtXR was subjected to different pH environments to see the effect of pH on enzymatic activity. Here, we covered a broad range of buffer conditions from extremely acidic to extremely basic pH environments. Buffers used in this study were glycine−HCl (2.0−3.0), sodium acetate buffer (4.0−5.5), phosphate buffer (6−7.5), Tris buffer (7−8.5), sodium bicarbonate buffer, and glycine NaOH buffer basic range. All of the samples with different pH buffers were prepared in triplicates. The samples were incubated for 4−6 h at room temperature (25 °C) before spectroscopic measurements.

3.7. Circular Dichroism (Far-UV CD) Measurements. The variations in secondary and tertiary structural signatures were determined using a Jasco J-815 spectropolarimeter. The enzyme was diluted to concentrations of 0.2 and 0.50 mg mL^{-1} in 20 mM sodium phosphate buffer (pH 7.0) for far-UV (200−250 nm) CD spectra. A cuvette with a 1 mm path length was used for far-UV measurements. The scanning speed was maintained at 10 nm min^{-1} for far-UV and 50 nm min^{-1} for near-UV measurement, and the spectrum was obtained by baseline correction with buffer. The variations in CD spectra were recorded at all temperatures at which deactivation profiles had been previously checked.

The raw CD data (θ_λ, T) were reduced to a concentration-independent parameter, the mean residue ellipticity, $[\theta]_\lambda$ (deg cm^2 dmol^{-1}), using the following relation

$$[\theta]_\lambda = \frac{M_{\text{o}}\theta_\lambda}{10lc} \quad (8)$$

where θ_λ is the observed ellipticity in millidegrees at wavelength λ; M_{o} is the mean residue weight of the protein; c is the concentration of TtXR in mg mL^{-1}; and l is the path length of the cell in centimeters.

3.8. Isothermal Titration Calorimetry (ITC). To evaluate the thermodynamic parameters and binding interaction of xylose reductase with ligand molecule (xylose) in the buffer solution, ITC was used. ITC is an excellent method to elucidate binding interaction, for which a VP-ITC calorimeter (MicroCal, 22 Industrial Drive East, Northampton, MA 01060, United States) apparatus was utilized.[44] The experiments were

https://doi.org/10.1021/acsomega.2c05690
ACS Omega 2022, 7, 44241−44250

carried out at 25 °C at pH 7.0 using 25 mM phosphate buffer, and the calorimeter cell was injected with a 30 μM protein solution (TtXR). The ligand (900 μM) was filled in a syringe and titrated in the cell containing the protein of interest with each injection of 10 μL except for the first injection of 5 μL, which was considered a false one, with 260 s interval with constant stirring at 316 rpm. The spacing was set and the data were normalized against the results of titration of ligand to TtXR and were evaluated by the MicroCal Origin ITC software, by a three-step sequential binding model as reported earlier[45] which could fit the data to generate the change in binding enthalpy (ΔH), change in entropy (ΔS) and the association constant (K_a). By these primary measurements, the secondary parameter change in Gibbs free energy (ΔG°) can be calculated by the following relation:

$$\Delta G^\circ = -RT \ln K_a = \Delta H - T\Delta S \quad (9)$$

where R is the gas constant and T is the absolute temperature.

The heat of dilution of the ligand in phosphate buffer was subtracted from the titration data. MicroCal Origin 8.0 was used to calculate the stoichiometry of the association constant (K_a), enthalpy change (ΔH), and binding (n).

4. CONCLUSIONS

The pentose sugar D-xylose is the predominant hemicellulosic compound, which comprises about one-third (25−35%) of the total carbohydrates present in the lignocellulosic biomass, which remains unutilized due to a lack of an optimized enzymatic method of xylose metabolism. Lignocellulose is renewable, and this low-cost carbohydrate is potentially attractive for producing useful chemicals (xylitol) and biofuel (bioethanol). The large-scale manufacturing of ethanol necessitates the efficient conversion of xylose from lignocellulosic feedstock. Thermostable organisms can be a potential source of thermostable enzymes for commercial and scientific interests. Therefore, *T. thermophilus* (a thermophile fungus) is explored as the alternative source of the thermostable enzyme xylose reductase. After heterologous expression in *E. coli*, purification of the native form of xylose reductase, which is thermostable, was done for the first time. Finally, the biochemical characterization of xylose reductase at different pH and temperature conditions was enumerated using various biophysical techniques. This study summarizes current information regarding yeast xylose reductases and the many ways used to provide an environmentally benign and long-term alternative source of XR for lignocellulose biomass consumption at higher temperatures in the fermentation sector. This study concludes that as far as its activity is concerned, xylose reductase works best around pH 7 and 45 °C. This information is very useful for industry as the temperature of fermenters containing heat-treated lignocellulose biomass is usually high and frequently affects the percentage yield of the final product.

ASSOCIATED CONTENT

Supporting Information

The Supporting Information is available free of charge at https://pubs.acs.org/doi/10.1021/acsomega.2c05690.

Expression pattern at two different temperatures: SDS-PAGE profile of cell lysates obtained after incubation for 5 h at 37 °C temperature (lanes 1−4: crude cell lysate TtXR, lane 5: protein marker 10−180 kDa, and lanes 6−8: crude cell lysate (cells grown at 20 °C for 12 h)) (Figure S1); and SDS-PAGE profile (12%) showing the protein marker in lane 1 and imidazole elusions 50, 100, 150 mM in lanes 2, 3, and 4, respectively, and the last lane contains cell lysate with the protein of interest (Figure S2) (PDF)

AUTHOR INFORMATION

Corresponding Author

Asimul Islam − *Centre for Interdisciplinary Research in Basic Sciences, Jamia Millia Islamia, New Delhi 110025, India;* orcid.org/0000-0001-9060-7970; Phone: 00919312812007; Email: aislam@jmi.ac.in

Authors

Nabeel Ali − *Centre for Interdisciplinary Research in Basic Sciences, Jamia Millia Islamia, New Delhi 110025, India*

Ayesha Aiman − *Centre for Interdisciplinary Research in Basic Sciences, Jamia Millia Islamia, New Delhi 110025, India*

Anas Shamsi − *Centre for Interdisciplinary Research in Basic Sciences, Jamia Millia Islamia, New Delhi 110025, India;* orcid.org/0000-0001-7055-7056

Imtaiyaz Hassan − *Centre for Interdisciplinary Research in Basic Sciences, Jamia Millia Islamia, New Delhi 110025, India;* orcid.org/0000-0002-3663-4940

Mohammad Shahid − *Department of Basic Medical Sciences, College of Medicine, Prince Sattam bin Abdulaziz University, Al Kharj 11942, Kingdom of Saudi Arabia*

Naseem A. Gaur − *International Centre for Genetic Engineering and Biotechnology, New Delhi 110067, India*

Complete contact information is available at: https://pubs.acs.org/10.1021/acsomega.2c05690

Author Contributions

N.A.: conceptualization, writing—review and editing, analysis of data, and data curation; A.A.: writing, editing, and data curation; A.S.: data validation, resources, visualization, and writing—review and editing; M.S.: data validation, resources, visualization, and writing—review and editing; N.A.G.: conceptualization; I.H.: visualization, data validation, and writing—review and editing; and A.I.: methodology, investigation, data curation, supervision, visualization, writing—review and editing, formal analysis, project administration, and writing—original draft.

Notes

The authors declare no competing financial interest.

All data generated or analyzed during this study are included in this manuscript and Supporting Materials are attached to this article.

ACKNOWLEDGMENTS

This work was supported by the grant from the Indian Council of Medical Research ISRM/12/(127)/2020, and the Science and Engineering Research Board (SERB, CRG/2018/004641). The authors are grateful to the FIST Program (SR/FST/LSI-541/2012) and Jamia Millia Islamia (a Central University) for providing all of the necessary facilities to carry out this work. The authors acknowledge the College of Medicine and Deanship of Scientific Research, Prince Sattam bin Abdul-Aziz University, Alkharj, KSA for their continuous support to carry out this research.

REFERENCES

(1) Arcaño, Y. D.; García, O. D. V.; Mandelli, D.; Carvalho, W. A.; Pontes, L. A. M. Xylitol: A review on the progress and challenges of its production by chemical route. *Catal. Today* **2020**, *344*, 2−14.

(2) Zhou, C.-H.; Xia, X.; Lin, C.-X.; Tong, D.-S.; Beltramini, J. Catalytic conversion of lignocellulosic biomass to fine chemicals and fuels. *Chem. Soc. Rev.* **2011**, *40*, 5588−5617.

(3) (a) Yilmaz, N.; Atmanli, A. Sustainable alternative fuels in aviation. *Energy* **2017**, *140*, 1378−1386. (b) Chiaramonti, D.; Prussi, M.; Buffi, M.; Tacconi, D. Sustainable bio kerosene: Process routes and industrial demonstration activities in aviation biofuels. *Appl. Energy* **2014**, *136*, 767−774.

(4) Budzianowski, W. M. High-value low-volume bioproducts coupled to bioenergies with potential to enhance business development of sustainable biorefineries. *Renewable Sustainable Energy Rev.* **2017**, *70*, 793−804.

(5) (a) Yousuf, A.; Sannino, F.; Pirozzi, D.*Lignocellulosic Biomass to Liquid Biofuels*; Academic Press, 2019. (b) Zabed, H.; Sahu, J.; Boyce, A. N.; Faruq, G. Fuel ethanol production from lignocellulosic biomass: an overview on feedstocks and technological approaches. *Renewable Sustainable Energy Rev.* **2016**, *66*, 751−774.

(6) Zhao, Z.; Xian, M.; Liu, M.; Zhao, G. Biochemical routes for uptake and conversion of xylose by microorganisms. *Biotechnol. Biofuels* **2020**, *13*, No. 21.

(7) de Paula, R. G.; Antoniêto, A. C. C.; Ribeiro, L. F. C.; Srivastava, N.; O'Donovan, A.; Mishra, P.; Gupta, V. K.; Silva, R. N. Engineered microbial host selection for value-added bioproducts from lignocellulose. *Biotechnol. Adv.* **2019**, *37*, No. 107347.

(8) Jeffries, T. W.Utilization of Xylose by Bacteria, Yeasts, and Fungi. In *Pentoses and Lignin*; De Gruyter, 1983; pp 1−32.

(9) Cordova, L. T.; Lu, J.; Cipolla, R. M.; Sandoval, N. R.; Long, C. P.; Antoniewicz, M. R. Co-utilization of glucose and xylose by evolved *Thermus thermophilus* LC113 strain elucidated by 13C metabolic flux analysis and whole genome sequencing. *Metab. Eng.* **2016**, *37*, 63−71.

(10) Zhu, D.; Adebisi, W. A.; Ahmad, F.; Sethupathy, S.; Danso, B.; Sun, J. Recent development of extremophilic bacteria and their application in biorefinery. *Front. Bioeng. Biotechnol.* **2020**, *8*, No. 483.

(11) (a) Kadowaki, M. A. S.; Higasi, P. M. R.; de Godoy, M. O.; de Araujo, E. A.; Godoy, A. S.; Prade, R. A.; Polikarpov, I. Enzymatic versatility and thermostability of a new aryl-alcohol oxidase from *Thermothelomyces thermophilus* M77. *Biochim. Biophys. Acta, Gen. Subj.* **2020**, *1864*, No. 129681. (b) de Oliveira, T. B.; Rodrigues, A.Ecology of Thermophilic Fungi. In *Fungi in Extreme Environments: Ecological Role and Biotechnological Significance*; Springer Nature, 2019; pp 39−57.

(12) Balabanova, L.; Seitkalieva, A.; Yugay, Y.; Rusapetova, T.; Slepchenko, L.; Podvolotskaya, A.; Yatsunskaya, M.; Vasyutkina, E.; Son, O.; Tekutyeva, L.; Shkryl, Y. Engineered Fungus *Thermothelomyces thermophilus* Producing Plant Storage Proteins. *J. Fungi* **2022**, *8*, No. 119.

(13) Cadete, R. M.; Rosa, C. A. The yeasts of the genus Spathaspora: potential candidates for second-generation biofuel production. *Yeast* **2018**, *35*, 191−199.

(14) Kumar, B.; Bhardwaj, N.; Agrawal, K.; Chaturvedi, V.; Verma, P. Current perspective on pretreatment technologies using lignocellulosic biomass: An emerging biorefinery concept. *Fuel Process. Technol.* **2020**, *199*, No. 106244.

(15) Bertels, L.-K.; Murillo, L. F.; Heinisch, J. J. The pentose phosphate pathway in yeasts−more than a poor cousin of glycolysis. *Biomolecules* **2021**, *11*, No. 725.

(16) Ahuja, V.; Macho, M.; Ewe, D.; Singh, M.; Saha, S.; Saurav, K. Biological and pharmacological potential of xylitol: a molecular insight of unique metabolism. *Foods* **2020**, *9*, No. 1592.

(17) Pileidis, F. D.; Titirici, M. M. Levulinic acid biorefineries: new challenges for efficient utilization of biomass. *ChemSusChem* **2016**, *9*, 562−582.

(18) Fatma, S.; Hameed, A.; Noman, M.; Ahmed, T.; Shahid, M.; Tariq, M.; Sohail, I.; Tabassum, R. Lignocellulosic biomass: a sustainable bioenergy source for the future. *Protein Pept. Lett.* **2018**, *25*, 148−163.

(19) Hu, Y.; Yu, D.; Wang, Z.; Hou, J.; Tyagi, R.; Liang, Y.; Hu, Y. Purification and characterization of a novel, highly potent fibrinolytic enzyme from Bacillus subtilis DC27 screened from Douchi, a traditional Chinese fermented soybean food. *Sci. Rep.* **2019**, *9*, No. 9235.

(20) Capece, A.; Romaniello, R.; Siesto, G.; Romano, P. Conventional and non-conventional yeasts in beer production. *Fermentation* **2018**, *4*, No. 38.

(21) Padilla, B.; Gil, J. V.; Manzanares, P. Challenges of the non-conventional yeast Wickerhamomyces anomalus in winemaking. *Fermentation* **2018**, *4*, No. 68.

(22) Questell-Santiago, Y. M.; Yeap, J. H.; Amiri, M. T.; Le Monnier, B. P.; Luterbacher, J. S. Catalyst evolution enhances production of xylitol from acetal-stabilized xylose. *ACS Sustainable Chem. Eng.* **2020**, *8*, 1709−1714.

(23) Schägger, H. Tricine−sds-page. *Nat. Protoc.* **2006**, *1*, 16−22.

(24) Garg, V. K.; Avashthi, H.; Tiwari, A.; Jain, P. A.; Ramkete, P. W.; Kayastha, A. M.; Singh, V. K. MFPPI−multi FASTA ProtParam interface. *Bioinformation* **2016**, *12*, 74−77.

(25) (a) Thambirajah, J.; Zulkali, M.; Hashim, M. Microbiological and biochemical changes during the composting of oil palm empty-fruit-bunches. Effect of nitrogen supplementation on the substrate. *Bioresour. Technol.* **1995**, *52*, 133−144. (b) Khanahmadi, M.; Arezi, I.; Amiri, M.-s.; Miranzadeh, M. Bioprocessing of agro-industrial residues for optimization of xylanase production by solid-state fermentation in flask and tray bioreactor. *Biocatal. Agric. Biotechnol.* **2018**, *13*, 272−282.

(26) Madeira-Jr, J. V.; Gombert, A. K. Towards high-temperature fuel ethanol production using Kluyveromyces marxianus: On the search for plug-in strains for the Brazilian sugarcane-based biorefinery. *Biomass Bioenergy* **2018**, *119*, 217−228.

(27) (a) Bhatti, Z. A.; Rajput, M.-U.-H.; Maitlo, G.; Solangi, Z. A.; Shaikh, G. S. Impact of storage time, rain and quality of molasses in the production of bioethanol. *Mehran Univ. Res. J. Eng. Technol.* **2019**, *38*, 1021−1032. (b) Soomro, A. F.; Abbasi, I. A.; Ni, Z.; Ying, L.; Liu, J. Influence of temperature on enhancement of volatile fatty acids fermentation from organic fraction of municipal solid waste: synergism between food and paper components. *Bioresour. Technol.* **2020**, *304*, No. 122980.

(28) Antosiewicz, J. M.; Shugar, D. UV−Vis spectroscopy of tyrosine side-groups in studies of protein structure. Part 2: Selected applications. *Biophys. Rev.* **2016**, *8*, 163−177.

(29) Ku, T.; Lu, P.; Chan, C.; Wang, T.; Lai, S.; Lyu, P.; Hsiao, N. Predicting melting temperature directly from protein sequences. *Comput. Biol. Chem.* **2009**, *33*, 445−450.

(30) Pace, C. N.; Scholtz, J. M.Measuring the Conformational Stability of a Protein. In *Protein Structure: A Practical Approach*; Oxford University Press: New York, 1997; Vol. *2*, pp 299−321.

(31) Miotto, M.; Olimpieri, P. P.; Di Rienzo, L.; Ambrosetti, F.; Corsi, P.; Lepore, R.; Tartaglia, G. G.; Milanetti, E. Insights on protein thermal stability: a graph representation of molecular interactions. *Bioinformatics* **2019**, *35*, 2569−2577.

(32) Kelly, S. M.; Jess, T. J.; Price, N. C. How to study proteins by circular dichroism. *Biochim. Biophys. Acta, Proteins Proteomics* **2005**, *1751*, 119−139.

(33) Shukla, H.; Shukla, R.; Sonkar, A.; Tripathi, T. Alterations in conformational topology and interaction dynamics caused by L418A mutation leads to activity loss of Mycobacterium tuberculosis isocitrate lyase. *Biochem. Biophys. Res. Commun.* **2017**, *490*, 276−282.

(34) Shahid, S.; Ahmad, F.; Hassan, M. I.; Islam, A. Relationship between protein stability and functional activity in the presence of macromolecular crowding agents alone and in mixture: An insight into stability-activity trade-off. *Arch. Biochem. Biophys.* **2015**, *584*, 42−50.

(35) Tripathi, T.; Röseler, A.; Rahlfs, S.; Becker, K.; Bhakuni, V. Conformational stability and energetics of Plasmodium falciparum glutaredoxin. *Biochimie* **2010**, *92*, 284−291.

https://doi.org/10.1021/acsomega.2c05690
ACS Omega 2022, 7, 44241−44250

(36) (a) Tripathi, T. Calculation of thermodynamic parameters of protein unfolding using far-ultraviolet circular dichroism. *J. Proteins Proteomics* **2013**, *4*, 85−91. (b) Anand, U.; Jash, C.; Mukherjee, S. Protein unfolding and subsequent refolding: a spectroscopic investigation. *Phys. Chem. Chem. Phys.* **2011**, *13*, 20418−20426.
(37) Shamsi, A.; Anwar, S.; Mohammad, T.; Alajmi, M. F.; Hussain, A.; Rehman, M.; Hasan, G. M.; Islam, A.; Hassan, M. MARK4 inhibited by AChE inhibitors, donepezil and Rivastigmine tartrate: Insights into Alzheimer's disease therapy. *Biomolecules* **2020**, *10*, No. 789.
(38) (a) Tu, Z.; He, G.; Li, K. X.; Chen, M. J.; Chang, J.; Chen, L.; Yao, Q.; Liu, D. P.; Ye, H.; Shi, J. An improved system for competent cell preparation and high efficiency plasmid transformation using different *Escherichia coli* strains. *Electron. J. Biotechnol.* **2005**, *8*, 113−120. (b) Hanahan, D. Studies on transformation of *Escherichia coli* with plasmids. *J. Mol. Biol.* **1983**, *166*, 557−580. (c) Chang, A. Y.; Chau, V.; Landas, J. A.; Pang, Y. Preparation of calcium competent *Escherichia coli* and heat-shock transformation. *JEMI methods* **2017**, *1*, 22−25.
(39) Pugh, M. E.; Schultz, E. Assessment of the purification of a protein by ion exchange and gel permeation chromatography. *Biochem. Mol. Biol. Educ.* **2002**, *30*, 179−183.
(40) Laemmli, U. K. Cleavage of structural proteins during the assembly of the head of bacteriophage T4. *Nature* **1970**, *227*, 680−685.
(41) (a) Jeppsson, M.; Träff, K.; Johansson, B.; Hahn-Hägerdal, B.; Gorwa-Grauslund, M. F. Effect of enhanced xylose reductase activity on xylose consumption and product distribution in xylose-fermenting recombinant Saccharomyces cerevisiae. *FEMS Yeast Res.* **2003**, *3*, 167−175. (b) Bruinenberg, P. M.; de Bot, P. H.; van Dijken, J. P.; Scheffers, W. A. NADH-linked aldose reductase: the key to anaerobic alcoholic fermentation of xylose by yeasts. *Applied Microbiol. Biotechnol.* **1984**, *19*, 256−260.
(42) (a) Quehenberger, J.; Reichenbach, T.; Baumann, N.; Rettenbacher, L.; Divne, C.; Spadiut, O. Kinetics and predicted structure of a novel xylose reductase from Chaetomium thermophilum. *Int. J. Mol. Sci.* **2019**, *20*, No. 185. (b) Kwon, D.-H.; Park, J.-B.; Hong, E.; Ha, S.-J. Ethanol production from xylose is highly increased by the Kluyveromyces marxianus mutant 17694-DH1. *Bioprocess Biosyst. Eng.* **2019**, *42*, 63−70.
(43) Verduyn, C.; Van Kleef, R.; Frank, J.; Schreuder, H.; Van Dijken, J.; Scheffers, W. Properties of the NAD (P) H-dependent xylose reductase from the xylose-fermenting yeast Pichia stipitis. *Biochem. J.* **1985**, *226*, 669−677.
(44) Khan, S.; Alhumaydhi, F. A.; Khan, M. S.; Sharaf, S. E.; Al Abdulmonem, W.; Hassan, M. I.; Shamsi, A.; Yadav, D. K. Exploring binding mechanism of naringenin to human transferrin using combined spectroscopic and computational methods: Towards therapeutic targeting of neurodegenerative diseases. *J. Mol. Liq.* **2022**, *356*, No. 119001.
(45) (a) Parray, Z. A.; Ahmad, F.; Alajmi, M. F.; Hussain, A.; Hassan, M. I.; Islam, A. Formation of molten globule state in horse heart cytochrome c under physiological conditions: Importance of soft interactions and spectroscopic approach in crowded milieu. *Int. J. Biol. Macromol.* **2020**, *148*, 192−200. (b) Parray, Z. A.; Ahmad, F.; Alajmi, M. F.; Hussain, A.; Hassan, M. I.; Islam, A. Interaction of polyethylene glycol with cytochrome c investigated via in vitro and in silico approaches. *Sci. Rep.* **2021**, *11*, No. 6475. (c) Parray, Z. A.; Ahmad, F.; Hassan, M. I.; Hasan, I.; Islam, A. Effects of Ethylene Glycol on the Structure and Stability of Myoglobin Using Spectroscopic, Interaction, and In Silico Approaches: Monomer Is Different from Those of Its Polymers. *ACS Omega* **2020**, *5*, 13840−13850.

https://doi.org/10.1021/acsomega.2c05690
ACS Omega 2022, 7, 44241−44250